Ground-penetrating radar data analysis for more complete archaeological interpretations

Lawrence B. Conyers[a]

KEY-WORDS: ground-penetrating radar, reflection profiles, reflection traces, GPR interpretation

GPR DATA PROCESSING TODAY

The use of GPR for archaeological mapping and interpretation has changed from its roots as a purely exploratory technique into one that uses sophisticated three-dimensional mapping and computer generated visualization programs to understand much larger areas of the subsurface (Conyers 2013). The standard visualization techniques today commonly produce amplitude slice-maps from two-dimensional reflection profiles or three-dimensional antenna arrays, generate isosurface renderings from those complex three-dimensional datasets, and generate a number of other three-dimensional outputs (Conyers and Leckebusch 2010; Novo *et al.* 2008; Trinks *et al.* 2010). These now common collection and processing techniques are the result of robust and easily accessible hardware and software advances that collect and process large datasets quickly and efficiently. While these advances are now common it is still important to understand and interpret the basic GPR data that are reflection traces and individual profiles. Only when all GPR information is interpreted together can the complex three-dimensional aspects of the method be understood. A few examples are presented here to illustrate how a visualization of uncorrected profiles used in slice-mapping can often produce erroneous images of layered ground. Buried features of interest also may not reflect radar energy and only an analysis of what is not reflecting waves will identify units of interest. In addition, an analysis of individual reflection traces , which are the most basic of datasets in GPR, will allow a determination of the types of materials in the ground that are producing the reflection.

SOME GPR EXAMPLES OF HOLISTIC INTERPRETATIONS FROM BASIC DATASETS

If the geological materials in the ground are complexly bedded, the computer sampling methods for amplitude mapping will display reflection amplitudes from one continuous horizon, as if it was a series of aerially restricted "anomalies" at various depths within each slice. As the layers in the ground are dipping, most GPR processing software used to generate three-dimensional images will generate extraordinarily busy "anomaly" maps that are mostly irrelevant to the final interpretation as slices cross horizons at various depths. Then the amplitude maps image only bedding horizons that may be located in any one slice (Fig. 1). Any archaeological features within this package of bedded material will be effectively hidden within the final images. In this case, only an understanding of the basic reflection information from which the images are produced within a geological context (Conyers 2015a) will allow an accurate final product.

[a] Department of Anthropology, University of Denver, Denver, Colorado, USA

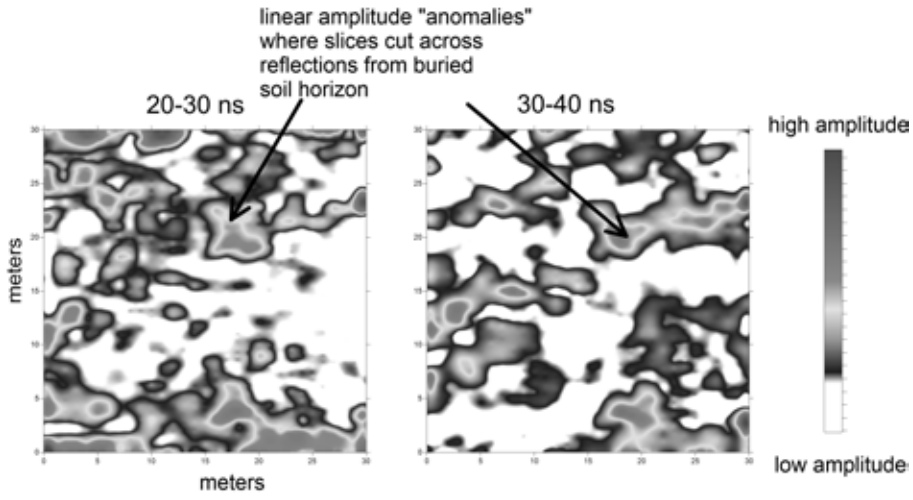

Fig. 1. Results of amplitude slice-mapping from 61 reflection profiles in a grid of depth slices, where amplitudes that appear to be aerially discrete reflections from that one horizon are plotted

Another basic question with GPR interpretation (Conyers 2012) is what may be producing the reflections in a dataset. Often this can be determined only from viewing reflections in profiles and understanding what produces radar reflections and then correlating those directly to the excavations or other information about the ground (Conyers 2015b). These basic interpretations make sense when the interfaces between archaeological materials and surrounding sediments and soils that produce the high amplitude reflections can be understood. In an area with buried homogeneous clay walls and floors, only the horizontal floors are visible in GPR profiles with the walls being non-reflective as they are composed of clay and other fine-grained materials with no interior bedding planes or other interfaces from with to reflect energy (Fig. 2). Any vertical interfaces between the walls and surrounding materials are also not reflective, as radar waves transmitted from the surface move parallel to these vertical boundaries; also if they intersect the interfaces, they are reflected away from the surface recording antenna and not recorded. When viewed in reflection profiles, the vertical clay walls appear as areas of no reflection and unless an interpreter understands the nature of the materials in the ground, these features will often go unnoticed.

Only after the houses are abandoned and the walls eroded, will the stratigraphy adjacent to the walls, composed of eroded walls, be visible. In this case, an understanding of the ground materials and what produces reflections will allow for an interpretation of the generated amplitude slice-maps. In these maps, it is the non-reflective areas that are denoting the buried walls, which are often not visible to the human eye without first integrating profile interpretations with amplitude maps

The basic dataset from which all GPR images are produced are the individual wave traces (Fig. 3). These are most often stacked along antenna transect lines to produce reflection profiles, and rarely do interpreters analyze them individually. For some applications the individual traces can be of great use in the interpretation to determine the physical properties of materials in the ground (Conyers 2012).

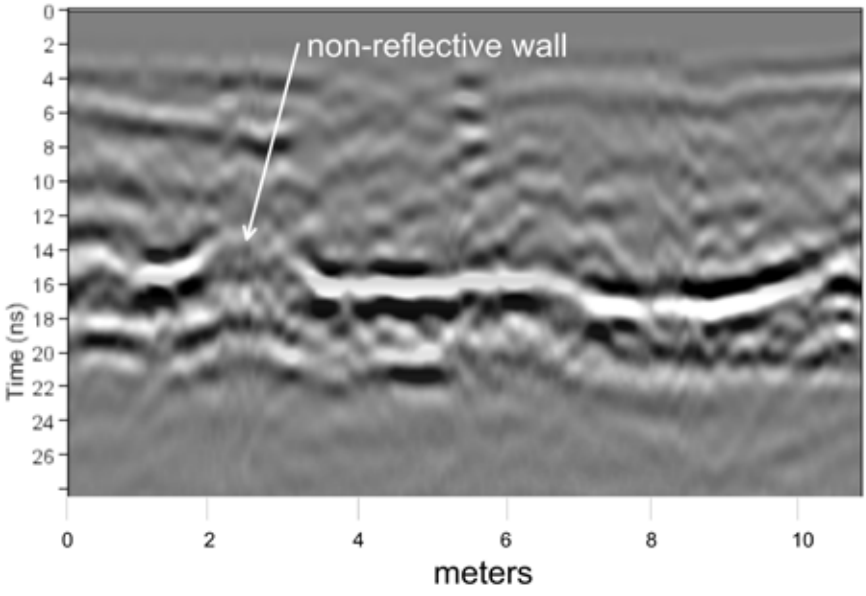

Fig. 2. Reflection profile perpendicular to an adobe wall that is non-reflective, with highly reflective adjacent "adobe melt" layers deposited on a buried living surface

When oscillating radar waves encounter buried interfaces, the waves change velocity and reflection occurs. In most ground, as radar energy moves deeper into the ground, moisture retention increases and radar travel velocity will decrease. When radar energy is reflected from a buried interface where the wave velocity decreases in the lower unit along the boundary, the polarity of the reflected wave will be the same as the direct-wave generated from the transmitting antenna (Fig. 3). This is termed normal polarity. However, if there is an increase in velocity along a boundary, such as an underground void space, the reflection generated will display a reversed polarity sine wave (Damiata *et al.* 2013). These types of polarity changes will occur not only when void spaces are encountered, but also when any buried material in the ground allows energy to increase in velocity rather than decrease. One very important, but often neglected aspect of GPR interpretation is this study of the polarity of individual waves generated from different materials. Usually amplitude slice-maps do not plot the polarity of the waves, but only their amplitude, and therefore an analysis of individual traces is necessary.

CONCLUSIONS

While amplitude slice-maps and isosurface renderings have revolutionized the way GPR data are presented, an accurate interpretation of those images often necessitates integration with more standard data analysis derived from reflection profiles and individual traces. The complexity of stratigraphic interfaces in the ground and changes in topography and surface materials can produce amplitude "anomalies" in the ground that are a function of the way data are resampled

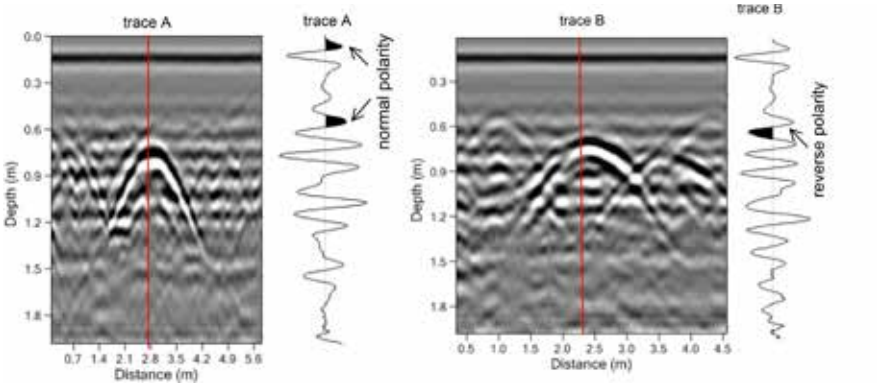

Fig. 3. Comparison of reflection traces from waves reflected from two graves. In burials that retain void spaces within caskets, reflections are reversed polarity (trace B). The usual case for most buried materials is to produce reflections that are normal polarity (trace A).

during processing. Only when profiles can be adjusted for these common variations, will the amplitude images be interpretable. While the common GPR processing steps move through a series of computing steps to the final products, users should often step back to the raw data, or the simplest images of reflections as a way to interpret the slice-maps and isosurfaces. Some may consider this integrative interpretation method "old fashioned", as this is the way most GPR reflections were processed prior to the now-common amplitude images, an understanding of intuitively generated reflection profiles and traces can produce important clues during interpretation tasks.

REFERENCES

Conyers, L. B. 2012. *Interpreting Ground-penetrating Radar for Archaeology.* Left Coast Press, Walnut Creek, California.

Conyers, L. B. 2013. *Ground-penetrating Radar for Archaeology.* Third Edition. Rowman and Littlefield Publishers, Alta Mira Press, Latham, Maryland

Conyers, L. B. 2015a. *Ground-penetrating Radar for Geoarchaeology.* Wiley-Blackwell Publishers, London.

Conyers, L. B. 2015b. Multiple GPR datasets for integrated archaeological mapping. *Journal of Near-surface Geophysics* 13 (3).

Conyers, L. B. and Leckebusch, J. 2010. Geophysical archaeology research agendas for the future: Some ground-penetrating radar examples. Archaeological Prospection 17: 117-123.

Damiata, B. N., Sternberg, John M., Bolender, Douglas J. Bolender and Zoëga, Guðný. 2013. Imaging skeletal remains with ground-penetrating radar: comparative results over two graves from Viking Age and Medieval churchyards on the Stóra-Seyla farm, northern Iceland. *Journal of Archaeological Science* 40: 268-278.

Novo, A., Grasmueck, M., Viggiano, D.A. and Lorenzo, H. 2008. 3D GPR in archaeology: what can be gained from dense data acquisition and processing? In *Proceedings, 12th International Conference on Ground Penetrating Radar (GPR 2008)*, Birmingham: 16-19.

Trinks, I., Johansson, B., Gustafsson, J., Emilsson, J., Friborg, J., Gustafsson, Ch.,

Nissen, J. and Hinterleitner, A. 2010. Efficient, large-scale archaeological prospection using a true three-dimensional ground-penetrating radar array system. *Archaeological Prospection* 17: 175-186.

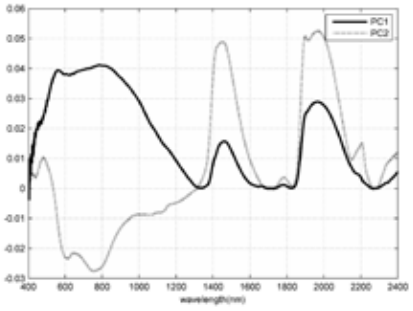

Fig. 1. Intensity of the first (PC1) and second (PC2) principal component

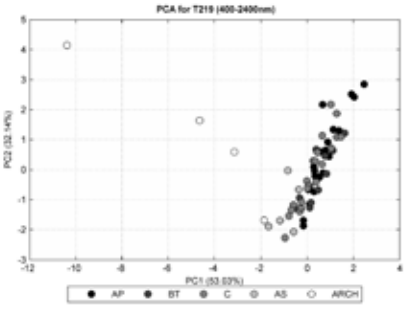

Fig. 2. PC1–PC2 plotting with different soil horizons. AP – distinct topsoil disturbed by ploughing: BT – B horizon (subsoil) enriched with clay; C – underlying unconsolidated material (parent material). AS –archaeological horizon; ARCH – archaeological material (burned soil and ceramics)

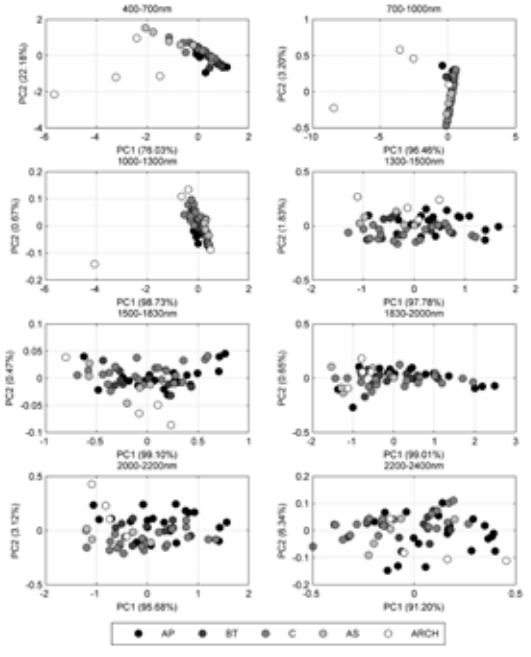

Fig. 3. PC1–PC2 plot at different wavelengths. AP – distinct topsoil disturbed by ploughing; BT – B horizon (subsoil) enriched in clay; C underlying unconsolidated material (parent material). AS – archaeological layer; ARCH – archaeological material (burned soil and potsherds).

length ranges are chosen according to various factors which affected the measurement. The separation of wavelength windows was performed at the spectrometer boundaries (ASD spectrometer is comprised of the different spectrometers) and close to strong water absorption bands. Since the archaeological horizon was visually distinguishable, we expected to see a clear separation between archaeological features and natural soil in the visible spectral range (400–700 nm). However, despite the small difference between archaeological materials and natural soil, PC1 does not make a clear separation. Also, the different horizons (which were seen visually) are not very well separated in the visible range. This is probably related to the normalisation procedure applied to the spectra. By looking at the PCA at different wavelengths, we can see that the archaeological materials (ARCH) are separated for wavelength ranges below 1000 nm. Beyond this wavelength, it becomes difficult to find the difference between archaeological material and natural soil.

CONCLUSION

The paper shows preliminary result of PCA application to the reflection spectra of archaeological remains. The result indicates that archaeological materials are well separated from the natural soil through PCA. The PCA result can probably be improved by using a larger dataset (spectra) over a wide range of archaeological sites. This will improve the statistical results and perhaps be used to separate different horizons as well. Currently, more research is going on with the PCA application to archaeological sites to distinguish archaeological remains through spectroscopy.

ACKNOWLEDGEMENTS

We extend our thanks to the University of Groningen and the National Museum of Hungary for their help and support during the fieldwork.

REFERENCE

Clark, R.N. and Roush, T.L. 1984. Reflectance Spectroscopy: Quantitative Analysis Techniques for Remote Sensing Applications. J*ournal of Geophysical Research* 89: 6329–6340.

Galvão, L.S., Pizarro, M. A. and Epiphanio, J.C.N. 2001. Variations in reflectance of tropical soils: Spectral-chemical composition relationships from AVIRIS data. *Remote Sensing of Environment* 75: 245–255.

Smith, M.O., Johnson, P.E. and Adams, J.B. 1985. Quantitative determination of mineral types and abundances from reflectance spectra using principal components analysis. *Journal of Geophysical Research* 90: 797–804.

Viscarra Rossel, R.A., Cattle, S.R., Ortega, A. and Fouad Y. 2009. In situ measurements of soil colour, mineral composition and clay content by vis-NIR spectroscopy. *Geoderma* 150: 253–266.